Steady State Entanglement in the Mechanical Vibrations of Two Dielectric Membranes

Michael J. Hartmann[1,2,*] and Martin B. Plenio[2]

[1]*Physik Department I/T34, Technische Universität München, 85748 Garching, Germany*
[2]*Institute for Mathematical Sciences, Imperial College London, and QOLS, Blackett Laboratory, Imperial College London, SW7 2BW, United Kingdom*

(Received 12 June 2008; published 13 November 2008)

We consider two dielectric membranes suspended inside a Fabry-Perot cavity, which are cooled to a steady state via a drive by suitable classical lasers. We show that the vibrations of the membranes can be entangled in this steady state. They thus form two mechanical, macroscopic degrees of freedom that share steady state entanglement.

DOI: 10.1103/PhysRevLett.101.200503 PACS numbers: 03.67.Bg, 03.65.Ta, 07.10.Cm, 42.50.Wk

Introduction.—Optomechanical systems in which electromagnetic degrees of freedom couple to the mechanical motion of mesoscopic or even macroscopic objects are promising candidates for studying the transition of a macroscopic degree of freedom from the classical to the quantum regime. These systems can also be of considerable technological use, e.g., for improved displacement measurements [1] and the detection of gravitational waves [2]. Optomechanical devices have therefore attracted considerable attention in recent years and micromirrors have been cooled by radiation pressure [3]. In many setups, one of the end mirrors of a Fabry-Perot cavity undergoes a mechanical vibration and the coupling between cavity photons and the mirror motion emerges because the resonance frequency of the cavity depends on its length and hence on the position of the mirror. Recently, devices have been introduced in which the motion of a membrane that is inserted into a Fabry-Perot cavity formed by rigid mirrors couples to the cavity mode [4,5]. Whereas the ground state and hence the quantum regime has not yet been reached in experiments, this has been predicted to be achievable if the mechanical oscillation frequency is larger than the cavity linewidth [6], a regime that has recently been observed [7]. In the quantum regime, it is then interesting to explore entanglement in mechanical, i.e., macroscopic degrees of freedom [8–10]. Possibilities to entangle the motion of a cavity micromirror with the electromagnetic field in the cavity have thus been explored in various approaches [11–15].

Here, we consider a Fabry-Perot cavity with two dielectric membranes suspended in its interior (cf. Fig. 1) and assume that two cavity resonances are driven by external lasers. With suitable lasers the mechanical vibrations of the membranes are cooled and asymptotically driven into a steady state. We show that the mechanical vibrations of the two membranes can be entangled in this asymptotic state. Entanglement between mechanical oscillators has been discussed previously but was either only found in the transient regime [11] (not the steady state) or required either a drive with nonclassical light [12] or mechanical oscillators that had been precooled to very low temperatures [13]. In contrast, our scheme generates steady state entanglement between mechanical degrees of freedom by cooling them via radiation pressure which only uses classical light sources. Our approach is not restricted to the specific setup mentioned here but also applies to other devices with optomechanical couplings [3] between two mechanical and two cavity modes.

Model.—We consider a Fabry-Perot cavity with two dielectric membranes in its interior (cf. Fig. 1). In this setup the optical resonance frequencies of the cavity depend on the positions of the membranes and can be derived from the boundary conditions of the field in the cavity [16]. Let $-3L$ ($3L$) and q_1 (q_2) be the positions of the left (right) rigid mirror and the left (right) membrane and T the transmissivity of the membranes. We denote the field modes in the left, center, and right part of the cavity by u_1, u_2, and u_3. For a mode with wave number k, the boundary conditions read [16] $u_1(-3L) = u_3(3L) = 0$, $u_1(q_1 - 0) = u_2(q_1 + 0)$, $u_2(q_2 - 0) = u_3(q_2 + 0)$, $\frac{du_1(q_1-0)}{dz} - \frac{du_2(q_1+0)}{dz} = k\eta u_1(q_1)$, and $\frac{du_2(q_2-0)}{dz} - \frac{du_3(q_2+0)}{dz} = k\eta u_2(q_2)$, where $\eta = 2\sqrt{(1-T)/T}$. In analogy to [5], we make the ansatz $u_1 = A\sin(k(q+3L))$, $u_2 = B\cos(kq) + \tilde{B}\sin(kq)$, and $u_3 = C\sin(k(q-3L))$ and obtain the transcendental equation, $[\cos(3kL) - \eta\cos(kq_1)\sin(kq_1 + 3kL)] \times [\sin(3kL) + \eta\sin(kq_2)\sin(kq_2 - 3kL)] + [\cos(3kL) + \eta\cos(kq_2)\sin(kq_2 - 3kL)][\sin(3kL) + \eta\sin(kq_1) \times \sin(kq_1 + 3kL)] = 0$, from which the optical reso-

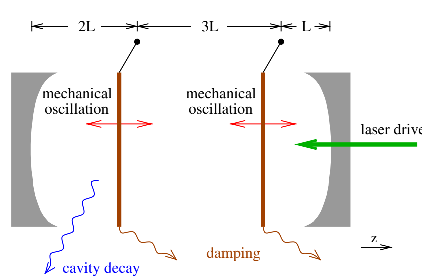

FIG. 1 (color online). The setup: Two mechanically vibrating membranes (brown) are suspended inside a Fabry-Perot cavity, which is driven by external lasers (green). Dissipation occurs via mechanical damping (brown) and cavity decay (blue).

nance frequencies $\omega = kc$ (c is the speed of light) can be found.

To obtain optomechancial coupling between two optical and two independent mechanical modes (see below), we choose the equilibrium positions of the membranes, q_{01} and q_{02}, to be $q_{01} = -L$ and $q_{02} = 2L$. For nonvibrating membranes, the optical resonance frequencies of the membrane cavity systems are then given by $\omega_{an} = \frac{n\pi c}{L}$, $\omega_{bn} = \frac{n\pi c}{L} - \frac{\theta c}{2L} + \frac{c}{2L}\cos^{-1}(-\frac{\cos\theta}{2})$, $\omega_{b'n} = \frac{n\pi c}{L} - \frac{\theta c}{2L} - \frac{c}{2L}\cos^{-1}(-\frac{\cos\theta}{2})$, and $\omega_{cm} = \frac{m\pi c}{3L} + \frac{\pi c}{6L} - \frac{\theta c}{3L}$, where n and m are positive integers. For membranes with low transmissivity, the frequencies ω_{an}, ω_{bn}, and ω_{cm} with $m = 3n$ lie close together, whereas $\omega_{b'n}$ is separated from this triplet and we thus focus on ω_{an}, ω_{bn}, and ω_{cm}.

In the case of vibrating membranes, the optical resonances depend on the motion of the membranes and their frequencies become functions of q_1 and q_2, e.g., $\omega_{an}(q_1, q_2)$. (The assumption that the optical resonances only depend on the membrane positions, not their momenta, is only valid if the membrane oscillations are much slower than the optical round-trip time, i.e., $\omega_m \ll |\omega_x - \omega_y|$ for $x, y = an, bn, cm$ [17], which we confirm below.) To obtain these functions, we write them as a power series up to linear order in the membrane positions, $\omega_x(q_1, q_2) = \omega_x(q_{01}, q_{02}) + \xi_{x1}(q_1 - q_{01}) + \xi_{x2}(q_2 - q_{02})$ for $x = an, bn, cm$ ($q_{01} = -L$ and $q_{02} = 2L$), expand the transcendental equation up to linear order in $q_j - q_{0j}$ ($j = 1, 2$), and solve it for zeroth and linear order separately to obtain $\omega_x(q_{01}, q_{02}) = \omega_x$, ξ_{x1}, and ξ_{x2} for $x = an, bn, cm$. For our choice of the membrane rest positions, $q_{01} = -L$ and $q_{02} = 2L$, the mode ω_{an} does not couple to the membrane motions, $\xi_{a1} = \xi_{a2} = 0$, and we discard it. The other couplings are $\xi_{b1} \approx (\frac{1}{10} + \frac{3}{400}T)\frac{n\pi c}{L^2}$, $\xi_{b2} \approx (\frac{2}{5} - \frac{39}{200}T)\frac{n\pi c}{L^2}$, and $\xi_{c1} = -\xi_{c2} \approx -(\frac{4}{45} - \frac{28}{675}T)\frac{m\pi c}{L^2}$ for $T \ll 1$ and $n, m \gg 1$. Higher order terms in the expansion of the frequencies give rise to additional coupling terms, also for ω_{an}, but these are negligible compared to the linear couplings. For symmetric membrane rest positions ($q_{01} = -L$, $q_{02} = L$), one would get $\xi_{b1} + \xi_{b2} = \xi_{c1} + \xi_{c2} = 0$ and the photons would only couple to the breathing mode, $q_1 - q_2$, whereas the center of mass mode, $q_1 + q_2$, would not be cooled. Note also the two optical modes are needed to cool two mechanical modes.

The corresponding Hamiltonian that describes the motion of the membranes and the cavity modes reads

$$H = \frac{\omega_m}{2}\sum_{j=1,2}(p_j^2 + q_j^2) + \sum_{x=bn,cm}\left(\frac{\Omega_x}{2}a_x + \text{H.c.}\right) + \sum_{x=bn,cm}\left(\Delta_x + \sum_{j=1,2}\xi_{xj}q_j\right)a_x^\dagger a_x, \tag{1}$$

where p_j and q_j are the momentum and position of membrane j ($j = 1, 2$). Both membranes have the same effective mass m and mechanical resonance frequency ω_m, and the optical modes with creation (annihilation) operators $a_{bn}^\dagger(a_{bn})$ and $a_{cm}^\dagger(a_{cm})$ are driven by classical lasers with Rabi frequencies Ω_{bn} and Ω_{cm}. We have redefined the position variables $q_j - q_{0j} \to q_j$ and write the optical modes in frames that rotate at the frequencies of their respective driving lasers, $\Delta_x = \omega_{x0} - \omega_{x,\text{laser}}$ [18]. In Eq. (1), we have also assumed that each laser only drives one cavity mode, which sets an upper bound to the permissible Rabi frequencies, $|\Omega_{bn}|, |\Omega_{cm}| \ll |\omega_{bn} - \omega_{cm}| \approx \frac{5}{12}c\sqrt{T}/L$ (to leading order in $T \ll 1$). This in turn limits the amount of entanglement that can be generated. The linear optomechanical couplings $\xi_{xj}q_j$ can be exploited to cool the membranes and drive them into a steady state. They furthermore generate entanglement between the mechanical vibrations via the optical modes as we will show.

Equations of motion.—Taking into account cavity decay and mechanical damping of the membranes, the Hamiltonian (1) gives rise to the Langevin equations [18],

$$\begin{aligned}\dot{a}_x &= -i\left(\Delta_x + \sum_{j=1,2}\xi_{xj}q_j - i\frac{\Gamma_x}{2}\right)a_x - i\frac{\Omega_x^\star}{2} + \sqrt{\Gamma_x}a_x^{\text{in}},\\ \dot{q}_j &= \omega_m p_j, \quad \dot{p}_j = -\omega_m q_j - \frac{\gamma}{2}p_j - \sum_x \xi_{xj}a_x^\dagger a_x + \zeta_j,\end{aligned} \tag{2}$$

where dots denote time derivatives and $[\cdot]^\star$ a complex conjugate. a_x^{in} and ζ_j are the optical and mechanical input noises and Γ_x and γ cavity decay and mechanical damping rates. The relevant nonzero correlation functions of the noise operators are $\langle a_x^{\text{in}}(t)(a_y^{\text{in}})^\dagger(t')\rangle = \delta_{xy}\delta(t - t')$ for $x, y = bn, cm$ and $\langle\zeta_j(t)\zeta_l(t')\rangle = \frac{\gamma}{2}(2n_{\omega_m} + 1)\delta_{jl}\delta(t - t')$ for $j, l = 1, 2$, where $n_{\omega_m} = [\exp(\hbar\omega_m/k_B\mathcal{T}) - 1]^{-1}$ is the thermal phonon number of the mechanical environment at temperature $\mathcal{T}$, k_B is Boltzmann's constant, and we have assumed $k_B\mathcal{T} \gg \hbar\omega_m$.

We split the operators in (2) into their steady state expectation values and quantum fluctuations, $a_x = c_x + \delta_x$, $p_j = P_j + \delta p_j$, and $q_j = Q_j + \delta q_j$. The constant steady state expectation values are given by the equations

$$\frac{\Omega_x^\star}{2} = -\left(\mu_x - i\frac{\Gamma_x}{2}\right)c_x, \qquad Q_j = -\sum_x \frac{\xi_{xj}}{\omega_m}|c_x|^2, \tag{3}$$

and $P_j = 0$, where $\mu_x = \Delta_x + \xi_{x1}Q_1 + \xi_{x2}Q_2$.

We are interested in a regime of high photon numbers in the cavity, in which the steady state expectation values are much larger than the quantum fluctuations. In this regime we can neglect all terms of higher than linear order in the fluctuations δ_x, δp_j, and δq_j in (2). (We have confirmed this approximation numerically.) The asymptotic state of the quantum fluctuations for the linearized equations is then a zero mean Gaussian state which is fully characterized by its covariance matrix $V_{ij} = 2\,\text{Re}\langle(O_i - \langle O_i\rangle) \times (O_j - \langle O_j\rangle)\rangle$, where $O = (\delta q_1, \delta p_1, \delta q_2, \delta p_2, X_{bn}, Y_{bn}, X_{cm}, Y_{cm})$ with $X_x = (\delta_x + \delta_x^\dagger)/\sqrt{2}$ and $Y_x = -i(\delta_x - \delta_x^\dagger)/\sqrt{2}$. We solve the linearized Langevin equations for the fluctuations to obtain the steady state covariance matrix V in the same way as in [14]. From V, the steady state entanglement as measured by the logarithmic negativity

E_N ($E_N \neq 0$ means the state is entangled) can then be computed [19] (see Ref. [20] for the technical details).

Steady state entanglement —We consider an example where both membranes have transmissivity $T = 0.2$, effective mass of $m = 10^{-9}$ g, and mechanical resonance frequency of $\omega_m = 10^6$ Hz [4]. The cavity is 6 mm long, hence $L = 1$ mm. For driving lasers of 1000 nm wavelength, the closest cavity modes have numbers $n = 2 \times 10^3$ and $m = 3n = 6 \times 10^3$. For these parameters, the optomechanical couplings attain the values $\xi_{bn,1} = 1.90$ kHz, $\xi_{bn,2} = 6.75$ kHz, and $\xi_{cm,1} = -\xi_{cm,2} = -4.53$ kHz. (We work in units, where δq_1 and δq_2 are dimensionless and given in multiples of $\sqrt{\hbar/(m\omega_m)}$.) Cooling to the quantum mechanical regime is possible if the mechanical oscillation frequency is larger than the optical linewidth [6,7] and we thus assume $\Gamma_{bn} = \Gamma_{cm} = \omega_m/10$. The mechanical Q is taken to be $Q = 10^7$, consistent with [4]. For the mechanical environment, we consider two temperature values, $\mathcal{T} = 8$ mK ($n_{\omega_m} = 1000$) and $\mathcal{T} = 100$ mK ($n_{\omega_m} = 13085$).

Figure 2 shows the entanglement of the two mechanical vibrations in the steady state measured by the logarithmic negativity E_N as a function of the steady state electromagnetic fields in the cavity, c_{bn} and c_{cm}. Since the Hamiltonian (1) only contains the photon numbers, the entanglement is insensitive to the phases of fields in the cavity and thus also to the phases of c_{bn} and c_{cm}. The linearization of Eq. (2) requires $|c_{bn}|, |c_{cm}| \gg 1$. In the left plot, we have $|c_{bn}| \sim 30$, but we also find $E_N = 0.195$ for $|c_{bn}| = 60$, $|c_{cm}| = 386.4$, $\Delta_{bn} = 4.2$ MHz, and $\Delta_{cm} = 20.9$ MHz. The values for Q and T, we assume here, are currently hard to achieve simultaneously, but the entanglement persists in a larger parameter range as shown in Fig. 3(d).

The Rabi frequencies Ω_{bn} and Ω_{cm} that are needed to generate the values of c_{bn} and c_{cm} in Fig. 2 are less than 11 GHz (left plot) and 23 GHz (right plot). The difference between the resonance frequencies ω_{bn} and ω_{cm} on the other hand is $|\omega_{bn} - \omega_{cm}| \approx 57$ GHz, and the separation of these two modes from other resonances is much larger, so that the lasers indeed only drive one resonance mode as assumed in Eq. (1). $|\omega_{bn} - \omega_{cm}| \propto L^{-1}$ so that $|\omega_{bn} - \omega_{cm}|$ would even be larger for a shorter cavity. By reducing the cavity length one could thus employ stronger driving lasers and create substantial entanglement even at higher $\mathcal{T}$. The input laser powers P_x are related to the Rabi frequencies by $P_x = \hbar\omega_{x,\mathrm{laser}}|\Omega_x|^2/(4\Gamma_x)$, which implies that laser powers between 0.6 pW and 60 μW are required. Furthermore, $\omega_m \ll |\omega_{bn} - \omega_{cm}|$ and the derivation of the cavity resonances and consequently the form of Hamiltonian (1) are well justified.

The steady states are furthermore characterized by phonon numbers of the vibration fluctuations, $n_j = \frac{1}{2}(\delta p_j^2 + \delta q_j^2 - 1)$, of $n_1 \leq 3, n_2 \leq 5$ for $\mathcal{T} = 8$ mK and $n_1 \leq 5$, $n_2 \leq 10$ for $\mathcal{T} = 100$ mK, and an entropy of the reduced density matrix of the vibrations, $S_m = -\mathrm{Tr}_{\mathrm{photons}}(\rho \log_2 \rho) \leq 4$, for both $\mathcal{T} = 8$ mK and $\mathcal{T} = 100$ mK. The steady state is thus indeed in the quantum regime. The linearized Langevin equations can be cast in matrix form $\dot{O} = OA + n$, where n is the vector of the noises [14]. Here, all eigenvalues of A have negative real parts below 1 kHz, which ensures that there is a unique steady state that is reached within milliseconds.

To further corroborate the robustness of the entanglement, we studied its dependence on fluctuations in the driving lasers and on variations in several system parameters. The results for $\mathcal{T} = 100$ mK are shown in Fig. 3. Figure 3(a) shows the dependence of E_N on the detunings of driving lasers, Δ_{bn} and Δ_{cm} ($c_{bn} = 60$ and $c_{cm} = 486$), Fig. 3(b) the dependence on the cavity decay rates Γ_{bn} and Γ_{cm}, Fig. 3(c) the dependence on the membranes resonance frequency ω_m and its effective mass m, and Fig. 3(d) the dependence of E_N on Q and $\mathcal{T}$.

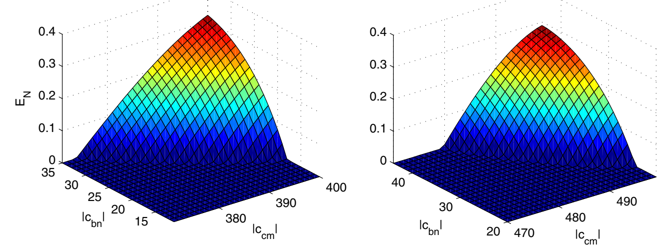

FIG. 2 (color online). The entanglement of the two mechanical vibrations in the steady state measured by the logarithmic negativity E_N as a function of c_{bn} and c_{cm}. Left plot: $\Delta_{bn} = 4.07$ MHz, $\Delta_{cm} = 20.84$ MHz, and $\mathcal{T} = 8$ mK ($n_{\omega_m} = 1000$). Right plot: $\Delta_{bn} = 6.12$ MHz, $\Delta_{cm} = 33.18$ MHz, and $\mathcal{T} = 100$ mK ($n_{\omega_m} = 13\,085$). The remaining parameters are $\omega_m = 1$ MHz, $m = 10^{-9}$ g, $T = 0.2$, $L = 1$ mm, $n = 2 \times 10^3$, $= 3n = 6 \times 10^3$, $q_{01} = -L$, $q_{02} = 2L$, $\Gamma_{bn} = \Gamma_{cm} = \omega_m/10$, and $Q = 10^7$ for both plots. Δ_{bn}, Δ_{cm}, c_{bn}, and c_{cm} have been optimized numerically for each case.

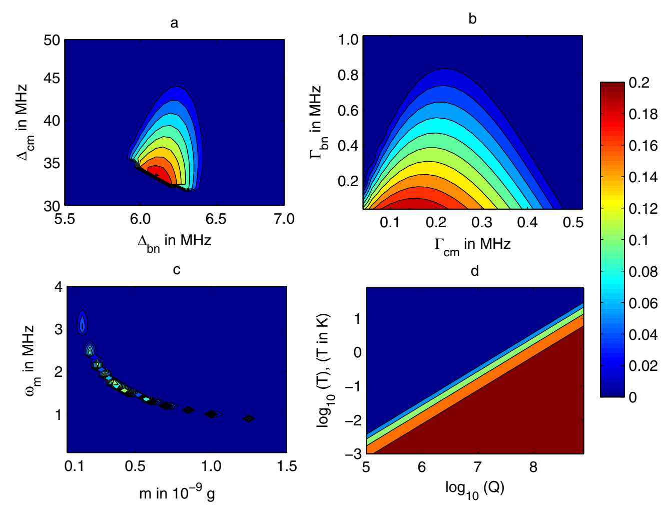

FIG. 3 (color online). The steady state entanglement of the two mechanical vibrations for $\mathcal{T} = 100$ mK, $c_{bn} = 60$, and $c_{cm} = 486$. (a) E_N as a function of Δ_{bn} and Δ_{cm}, (b) E_N as a function of Γ_{bn} and Γ_{cm}, (c) E_N as a function of m and ω_m, and (d) E_N as a function of Q and T. All other parameters as in Fig. 2.

dependence on the mechanical Q and the environment temperature $\mathcal{T}$. In all cases there is a substantial parameter region which shows entanglement. Note that we assign $E_N = 0$ to all points where there is no well-defined steady state due to heating, i.e., where an eigenvalue of A has a positive real part. Furthermore, our driving fields are optimized for the values in Fig. 2. For different values of Γ_{bn}, Γ_{cm}, Q, γ, ω_m, or m, slightly modified laser drives will yield more entanglement.

One can obtain some intuitive indications why the membrane vibrations become entangled. The Hamiltonian corresponding to the linearized Langevin equations for the fluctuations δp_1, δq_1, δp_2, δq_2, δ_{bn}, and δ_{cm} is $H = \frac{\omega_m}{2}\sum_j(\delta p_j^2 + \delta q_j^2) + \sum_x \mu_x \delta_x^\dagger \delta_x + \sum_{j,x}(\xi_{xj} c_x \delta q_j \delta_x^\dagger + \mathrm{H.c.})$. In the parameter regime of interest, we have $\mu_x \gg |\xi_{xj} c_x|$ and the photon degrees of freedom can be adiabatically eliminated to obtain the effective Hamiltonian $\mathcal{H} = \frac{\omega_m}{2}(\delta p_1^2 + \delta p_2^2) + \frac{\omega_m + \nu_1}{2}\delta q_1^2 + \frac{\omega_m + \nu_2}{2}\delta q_2^2 + \frac{\nu_{12}}{2}\delta q_1 \delta q_2$, where $\nu_j = -2\sum_x \xi_{xj}^2 |c_x|^2/\mu_x$ and $\nu_{12} = -4\sum_x \xi_{x1}\xi_{x2}|c_x|^2/\mu_x$. The ground state of $\mathcal{H}$ and hence states close to it are entangled in regimes where $|\nu_{12}| \sim \omega_m$ or larger, which is the case for the parameters in Fig. 2.

Entanglement verification.—To verify the created entanglement quantitatively in an experiment, several quadrature correlations need to be measured [9,21]. This may be achieved by employing at least two further weak probe lasers, similar in spirit to the scheme in [14], which drive cavity modes that do not participate in the entanglement generation, i.e., modes with $n \neq 2 \times 10^3$ or $m \neq 6 \times 10^3$. The equation of motion for the fluctuations of the probe field, δ_y, reads $\dot{\delta}_y = -i\mu_y \delta_y + \sqrt{\Gamma_y}\delta_y^{\mathrm{in}} - i\frac{c_y}{\sqrt{2}}(\xi_{y1}C_1 + \xi_{y2}C_2)$ in a frame that rotates at the frequency of the probe laser, ω_L. Here $\delta q_j = \frac{1}{\sqrt{2}}(C_j + C_j^\dagger)$ and we have assumed $|\xi_j c_y| \ll \omega_m$ and applied a rotating wave approximation. In a Fourier transformed picture in the laboratory frame this equation reads $-i(\omega - \mu_y)\delta_y(\omega) = \sqrt{\Gamma_y}\delta_y^{\mathrm{in}}(\omega) - i\frac{c_y}{\sqrt{2}}[\xi_{y1}C_1(\omega - \omega_L) + \xi_{y2}C_2(\omega - \omega_L)]$. Applying standard input-output formalism [18], $a_y^{\mathrm{out}}(\omega) = \sqrt{\Gamma_y}[c_y \delta(\omega - \omega_L) + \delta_y(\omega)] - [c_y^{\mathrm{in}}\delta(\omega - \omega_L) + \delta_y^{\mathrm{in}}]$, the output field is given by $a_y^{\mathrm{out}}(\omega) = -\frac{\omega - \mu_y - i\Gamma_y}{\omega - \mu_y}\delta_y^{\mathrm{in}}(\omega) + (\sqrt{\Gamma_y}c_y - c_y^{\mathrm{in}})\delta(\omega - \omega_L) + \frac{c_y}{\omega - \mu_y}\sqrt{\frac{\Gamma_y}{2}}[\xi_{y1}C_1(\omega - \omega_L) + \xi_{y2}C_2(\omega - \omega_L)]$, where c_y^{in} is the input field of the probe laser. The background terms c_y and c_y^{in} only contribute for $\omega = \omega_L$. Homodyne measurements on the output field thus allow one to measure $\xi_{y1}C_1(\omega - \omega_L) + \xi_{y2}C_2(\omega - \omega_L)$. The second probe laser on a mode with different ξ_{y1} and ξ_{y2} measures a different linear combination of C_1 and C_2 and hence a different quadrature. As the steady state of the membranes allows for repeated measurements, two probe lasers enable a reconstruction of the covariance matrix V, where the precision is limited by the input noise δ_y^{in} (see Ref. [20] for the technical details).

Conclusions.—The scheme presented here allows one to generate steady state entanglement of the motion of two dielectric membranes, which are suspended inside a Fabry-Perot cavity with a cavity decay rate that is lower than the mechanical resonance frequency of the membranes. The scheme only requires a drive by classical light and can work for environment temperatures up to a few kelvin. With increasing environment temperatures, stronger driving lasers and therefore shorter cavities with larger mode separation are needed. Measurements on the output fields of additional weak probe lasers can be used to verify the created entanglement.

M. J. H. thanks Ignacio Wilson-Rae for fruitful discussions. This work is part of the EPSRC QIP-IRC, the EU integrated project QAP, the Emmy Noether project HA 5593/1-1, and was supported by the EPSRC grant EP/E058256 and the Alexander von Humboldt foundation.

*michael.hartmann@ph.tum.de

[1] D. Rugar *et al.*, Nature (London) **430**, 329 (2004).
[2] V. Braginsky and S. P. Vyatchanin, Phys. Lett. A **293**, 228 (2002).
[3] O. Arcizet *et al.*, Nature (London) **444**, 71 (2006); S. Gigan *et al.*, Nature (London) **444**, 67 (2006); D. Kleckner and D. Bouwmeester, Nature (London) **444**, 75 (2006); A. Schliesser *et al.*, Phys. Rev. Lett. **97**, 243905 (2006).
[4] J. D. Thompson *et al.*, Nature (London) **452**, 72 (2008).
[5] M. Bhattacharya and P. Meystre, Phys. Rev. A **78**, 041801 (R) (2008); M. Bhattacharya, H. Uys, and P. Meystre, Phys. Rev. A **77**, 033819 (2008).
[6] M. Bhattacharya and P. Meystre, Phys. Rev. Lett. **99**, 073601 (2007); I. Wilson-Rae *et al.*, *ibid.* **99**, 093901 (2007); F. Marquardt *et al.*, *ibid.* **99**, 093902 (2007); C. Genes *et al.*, Phys. Rev. A **77**, 033804 (2008).
[7] A. Schliesser *et al.*, Nature Phys. **4**, 415 (2008).
[8] A. D. Armour, M. P. Blencowe, and K. C. Schwab, Phys. Rev. Lett. **88**, 148301 (2002).
[9] J. Eisert *et al.*, Phys. Rev. Lett. **93**, 190402 (2004).
[10] L. Tian and P. Zoller, Phys. Rev. Lett. **93**, 266403 (2004).
[11] S. Mancini *et al.*, Phys. Rev. Lett. **88**, 120401 (2002).
[12] M. Pinard *et al.*, Europhys. Lett. **72**, 747 (2005).
[13] D. Vitali, S. Mancini, and P. Tombesi, J. Phys. A **40**, 8055 (2007).
[14] D. Vitali *et al.*, Phys. Rev. Lett. **98**, 030405 (2007).
[15] M. Paternostro *et al.*, Phys. Rev. Lett. **99**, 250401 (2007).
[16] M. B. Spencer and W. E. Lamb, Phys. Rev. A **5**, 893 (1972).
[17] C. K. Law, Phys. Rev. A **51**, 2537 (1995).
[18] C. Gardiner and P. Zoller, *Quantum Noise* (Springer, New York, 2004).
[19] M. B. Plenio and S. Virmani, Quantum Inf. Comput. **7**, 1 (2007); M. B. Plenio, Phys. Rev. Lett. **95**, 090503 (2005); J. Eisert, Ph.D. thesis, University of Potsdam, 2001.
[20] See EPAPS Document No. E-PRLTAO-101-026847 for details of the derivations. For more information on EPAPS, see http://www.aip.org/pubservs/epaps.html.
[21] L.-M. Duan *et al.*, Phys. Rev. Lett. **84**, 2722 (2000).